INSTITUTE OF PLASMA PHYSICS
CZECHOSLOVAK ACADEMY OF SCIENCES

MODEL OF OXYGEN IONS RESONANT LINES EMISSION OF REB-HEATED PLASMA

J.Rauš, V.Babický

IPPCZ-294

June 1989

RESEARCH REPORT

POD VODÁRENSKOU VĚŽÍ 4, 18069 PRAGUE 8
CZECHOSLOVAKIA

MODEL OF OXYGEN IONS RESONANT LINES EMISSION OF REB-HEATED PLASMA

J.Rauš, V.Babický

IPPCZ 294 JUNE 1989

Abstract

Time dependent intensities of selected resonant lines of oxygen impurity in ionization stages O^{2+} - O^{5+} in hydrogen plasma of n_e about 10^{15} cm^{-3} are calculated by using nonstationary corona model with variable electron temperature of the maximum value of 20 - 50 eV (plasma parameters of REBEX experiment), to judge the possibilities of prepared measurements and to facilitate their interpretatiton. Simultaneously the rough form of XRD signals corresponding to these parameters and the influence of radiation losses on plasma decay are shown.

Introduction

Electron temperature of plasma bulk on REBEX experiment (hydrogen plasma heated by relativistic electron beam ~ 350 kV, 30 kA, 100 ns; resulting T_e of tens of eV) [1] was measured from the exponential slope of continuum spectra of plasma radiation in utrasoft X-ray region (10 eV - 1 keV) by filter method, using vacuum X-ray diodes (XRD) and submicrometer nitrocelulose filters [2]. Because the radiation spectrum is deformed by presence of impurities (in our case especially C, O, and Al; $n_{imp} \sim 1\% \, n_e$ deduced from the magnitude of XRD signal), sufficiently precise interpretation of such measurements can be made only in the case of low electron densities ($n_e \sim 10^{14}$ cm^{-3}), when the ionization times of impurities are so long, that their ionization state is sufficiently low to suppress the line emission even by the thinest filters during all the measured signals. For results interpretation in a general case, a model of radiation emission must be made, including time dependent density of individual ionization stages of all impurities and time dependent radiation spectrum (bremsstrahlung, recombination continuum and line emission).

Behaviour of our plasma ($n_e = 10^{14} - 10^{16}$ cm^{-3}, T_e tens of eV, beam injection time << hot plasma lifetime and characteristic ionization times) can be described by nonstacionary corona model. In our previous work [3], a set of calculations have been made for understanding the influence of different processes on our measurements. These calculations were made for 1% oxygen impurity in the constant T_e approximation, which was found to be not too bad for time conditions on REBEX (such calculations need substantially shorter computer times because of constant coefficients in dif. equations for ionization state and in spectrum calculations). It is seen from the results of this model, that by our plasma parameters about 90% of radiation power is emitted in the spectral range 10 - 25 eV due to resonant lines of the type 2s - 2p of all generated ionization stages $O^{1+} - O^{5+}$. Therefore, information on T_e can be obtained only from measurements with nitrocellulose filter thicker than ~ 0.15 µm. In Fig.1 and 2 theoretical XRD signal deduced from this model for $T_e = 40$ eV, $n_e = 10^{15}$ cm^{-3} and its reduction by filters of different thicknesses are shown, respectively. In some regimes of beam-plasma interaction, the form of experimental XRD signal is similar to that from Fig.1 for $t < 1$ µs, but a more typical experimental form is that shown in Fig.3. From measurements with filters (by the assumption that the dominant impurity is oxygen) (Fig.4) and from comparison with results of other diagnostic methods, the maximum T_e of 30 - 40 eV can be deduced in this concrete regime.

We have made also the first attempt at calculations with variable T_e [4]. The main result of this attempt is that decrease of T_e due to radiative energy losses at plasma parameters which can be achieved in REBEX machine is in relatively good agreement with the decay of plasma bulk deduced from diamagnetic mesurements [5] (according to our estimations, losses due to plasma diffusion to walls at such parameters are lower).

All the above mentioned calculations were made only for oxygen and only the most intensive resonant lines were taken into account. Similar calculations for other impurities are possible, but real percentual impurity composition is unknown. Precise spectra calculation including all possible lines in relatively large spectral range is out of our possibilities. Calculations of radiation losses, and consequently the decrease of T_e and the form of bare XRD signal in variable T_e model, are practically independent of these facts; but a more substantial influence can be achieved in calculations of XRD signal reduction by filters. Therefore, T_e measurements by filter method at plasma densities now under investigation on REBEX ($n_e \sim 10^{15}$ cm^{-3} and higher) can be used only for rough estimations. At present we prepare an experiment for measuring the time dependent intensities of resonant lines of $O^{2+} - O^{5+}$, which can give more information on time behaviour of T_e. The main purpose of the presented work is to make theoretical bases for these measurements.

2) 2s - 2p transitions of oxygen ions

The most intensive spectral lines of oxygen ions at our plasma parameters (about 90% of all intensity) are those of the type 2s - 2p. In Fig.5 - 9 the term structure of the ground configuration $1s^2 2s^k 2p^l$ and of the excited one

$1s^2 2s^{k-1} 2p^{l+1}$, and optically allowed radiative transitions between these configurations (with λ_{vac} in Å) are shown for the ionization stages of oxygen gene··ted in our plasma (O^{1+} to O^{5+}). These graphs were constructed by using the data of ref.[6–8].

In our previous calculations [3], according to standart calculations of radiation losses (e.g.[9–10]), only transitions to the ground state are taken into account. In the case of O^{4+} and O^{2+}, also intensive lines corresponding to the transitions to metastable state are observed [7,8] – Fig.5,6. For O^{2+}, transitions to the ground state are substantially predominant, but for O^{4+} transitions to the metastable states (which probably can be excited in our plasma) may enhance the radiation intensity (for discussion of influence of this fact see section 4).

For lines intensity measurements, such lines (or groups of lines) must be picked out, which can be (by the used monochromator) hopefully selected from the emitted radiation spectrum, i.e. close to which no lines of other ionization stages of oxygen or of other possible impurities exists. (especially C and Al). The concrete selection (using the tables [8]) is shown in Tab.1, simultaneously with parameters needed for intensity calculation (cf. section 3c). The lines of O^{1+} are not taken into account because of probable deformation of experimental results by plasma periphery.

3) Methods of calculation

a) Atomic processes

I o n i z a t i o n. In the corona model, only electron impact ionization from the ground state is taken into account (ionization by electrons from excited states, photoionization and autoionization are neglected with respect to the low plasma density). For $T_e < 50$ eV the ionization of O^{6+} to O^{7+} can be neglected as well as ionization of lower ionization stages from the K shell. Neutral oxygen is not taken into account, because $T_e > 3$ eV during all included processes. Therefore, only ionization of O^{1+} - O^{5+} from the L shell is included. The ionization rate coefficients for ionization of ions with charge Q are calculated by the following formula, constructed by using data from ref. [11,12] (in $cm^3 s^{-1}$):

$$S_Q = 10^{-6} a_Q T_e^{-3/2} \xi_Q \frac{E_i(I_Q/T_e)}{I_Q/T_e} ; \qquad Q = 1 \div 5 ,$$

where T_e is electron temperature in eV, ξ_Q is a number of "equivalent" electrons in the L shell, I_Q is the effective ionization potential from the L shell in eV (i.e. weighted average of $I_{2s}(Q)$ and $I_{2p}(Q)$, which are given by Lotz [13]), a_Q are individual constants (selected in such a way, that the resulting coefficients are in good agreement with those presented by Lotz [12]), and $Ei(x) = \int_x^\infty \frac{e^{-y}}{y} dy$ is the exponential integral. The needed parameters are shown in Tab.2.

R e c o m b i n a t i o n. For plasma parameters corresponding to the corona model, radiative and dielectronic recombination must be taken into account. For the radiative recombination rate coefficients we use the standard formula (cf. e.g. [9]) in the following form (in $cm^3 s^{-1}$):

$$R_Q = 1{,}2\cdot 10^{-4} Q^2 T_e^{-1/2}\Big[(8-\xi_Q)\frac{I_{Q-1}}{T_e}\, e^{I_{Q-1}/T_e}\, E_i(I_{Q-1}/T_e) + \sum_{n=3}^{15}\frac{21{,}76}{n^3}\,\frac{Q^2}{T_e}\, e^{\left(\frac{13{,}6\,Q^2}{n^2 T_e}\right)} E_i\left(\frac{13{,}6\,Q^2}{n^2 T_e}\right)\Big]; \quad Q = 2 \div 6,$$

where the first term represents recombination to the L shell ($8-\xi_Q$ is the number of empty places), while the second one that to the excited levels with principle quantum number $n \geq 3$, which are assumed to be hydrogenic. The free-bound Gaunt factor is taken equal to 1.

For dielectronic recombination, only the first resonant lines are included (of the type 2s - 2p; averaged over all terms when needed). The respective rate coefficients are given by the formula proposed by Vainshtein [14] (in $cm^3 s^{-1}$):

$$K_Q = 10^{-11} d_Q \left(\frac{E_Q}{T_e}\right)^{3/2} e^{-E_Q/T_e}; \quad Q = 2 \div 5,$$

where E_Q is the excitation energy of the transition in eV and d_Q are individual constants (taken from ref. [15]). All the needed parameters are given in Tab. 2. Density dependence of dielectronic recombination is neglected.

I o n i z a t i o n s t a t e. The time dependent ionization state of oxygen is given by the following differential equations (in our conditions):

$$\frac{dn_Q}{dt} = -n_e n_Q S_Q + n_e n_{Q+1}\left(R_{Q+1} + K_{Q+1}\right) \qquad Q=1$$

$$\frac{dn_Q}{dt} = -n_e n_Q \left(S_Q + K_Q + R_Q\right) + n_e n_{Q-1} S_{Q-1} + n_e n_{Q+1}\left(R_{Q+1} + K_{Q+1}\right) \qquad Q=2\div5$$

$$\frac{dn_Q}{dt} = -n_e n_Q \left(R_Q + K_Q\right) + n_e n_{Q-1} S_{Q-1} \qquad Q=6.$$

Here n_Q are the relative densities of oxygen ions with charge Q (in comparison with the total oxygen density n_0), n_e is electron density in cm^{-3} (which is assumed to be constant according to constant frequency of diamagnetic signal on REBEX; changes of n_e due to ionization of impurities are less then 10%). Because oxygen is practically in ionization state O^{4+} by forplasma $T_e \sim 3$ eV, the initial conditions for dif. equations are:

$$n_1(t=0)=1\,, \quad n_{Q+1}(t=0)=0.$$

Coeffitients S_Q, R_Q and K_Q are temperature dependent. Therefore, time dependence of T_e must be known for solving the above mentioned equations (see section 3b). In our calculations, these equations are solved numerically by using the Euler method.

Excitation; radiation losses. In the corona model an assumption is made, that line emission is caused by spontaneous decay of excited states generated by electron impact excitation from the ground state. In this work, only the first resonant transitions (of the type 2s - 2p) are included. The excitation rate coefficients are calculated by the following way (used for example by Tazima et al.[10]):

$$F_Q = 10^{-6} c_Q E_Q^{-3/2} \left(\frac{E_Q}{T_e}\right)^{1/2} e^{-E_Q/T_e} \quad (\text{in } cm^3 s^{-1}); \quad Q = 1 \div 5.$$

The respective transition energies E_Q (in eV, averaged over all terms when needed) and constants c_Q shown in Tab.2 were obtained by combining the data from ref.[9] and [10].

By plasma parameters used in this work, radiation losses due to bremsstrahlung and both radiative and dielectronic recombination can be neglected. In the line emission, the 2s - 2p lines are substantially predominant. The energy needed for ionization is also much smaller than that emitted in these lines. Therefore, losses due to "collisional and radiative processes" (ionization, recombination and radiation) can be represented by

$$P = n_0 \sum_{Q=1}^{5} n_Q F_Q E_Q .$$

Here P (in eVs^{-1}) are losses coming to one electron, n_o is oxygen density in cm^{-3}.

All the included lines fall in the spectral interval of the maximum sensitivity of XRD, 10 - 25 eV (about 10^{-2} A/W) [2]. The radiation losses are practically independent of the type of light impurity. Therefore, the rough form of bare XRD signal corresponding to the plasma parameters used in these calculations can be approximated by (including concrete conditions of our measurements):

$$XRD(t) = 1{,}8 \cdot 10^{-22} n_i P(t) \qquad \text{(in Volts)}.$$

b) Electron temperature

On the REBEX experiment, the forplasma of T_e of about 3 eV is heated by REB of the pulse duration $\sim$ 100 ns. After REB injection, the plasma bulk can be mildly heated by relaxation of a small group of overthermal electrons (which is generated during the REB-plasma interaction) and/or by dissipation of redistributed magnetic field [1]. The characteristic decay time of the overthermal component, deduced from diamagnetic measurements, is several hundreds of ns [5]. Therefore, time dependence of T_e in our calculations is approximated by the exponential function in such a way, that $T_{e\,max} = T_e(0{,}5\ \mu s) \sim 1{,}5\ T_e(0{,}1\ \mu s)$. According to our previous estimations, $T_{e\,max}$ of 20, 30 and 45 eV were selected. The respective analytical expressions of T_e are:

$$\left.\begin{aligned} T_{e1}(t) &= 17(1 - e^{-10^7 t}) + 3 \\ T_{e2}(t) &= 27(1 - e^{-10^7 t}) + 3 \\ T_{e3}(t) &= 42(1 - e^{-10^7 t}) + 3 \end{aligned}\right\} t \leq 5 \cdot 10^{-7}\,s ,$$

where t is time in s, T_e is in eV. For $t > 0{,}5\ \mu s$ we assume, that T_e decreases due to radiation losses (which are independent of the type of light impurity). Because the average electron energy is $\frac{3}{2} T_e$, electron temperature is expressed as $T_e(t_{i+1}) = T_e(t_i) - \frac{2}{3} \Delta t\, P(t_i)$; $t > 5 \cdot 10^{-7}\,s$.

Here $\Delta t = t_{i+1} - t_i$ is the time step in numerical calculations of differential equations for ionization state of oxygen.

The energy distribution of plasma bulk electrons is assumed to be maxwellian during all the above mentioned processes (influence of overthermal component is neglected).

c) Time dependence of lines intensity

The intensity of the selected spectral lines (or groups of lines) - see section 2 - is calculated in a way similar to that used for radiation losses due to line emission caused by electron impact excitation. The line intensity in Wcm^{-3} is given by

$$PL_Q = 10^{-25} b_Q n_e n_o n_Q T_e^{-1/2} e^{-W_Q/T_e} \; ; \quad Q = 2 \div 5 ,$$

where W_Q is the transition energy in eV and b_Q are individual constants. These parameters, as given by Tazima et al.[10], are shown in Tab.1. For O^{5+}, the constant b_Q is 0,5 of that used by Tazima for $2s^2S - 2p^2P$ transition, because only one line from the dublet of comparable intensities is selected for our measurements.

4) Results

Calculations are made for the following plasma parameters: Oxygen density is $n_0 = 2.10^{13}$ cm^{-3} according to the most probable value of density of impurities deduced from the magnitude of experimental XRD signals at REBEX. Electron density in present experiments at REBEX is about 10^{15} cm^{-3}. Therefore, calculations are made for three values of n_e, 5.10^{14}, 10^{15} and 2.10^{15} cm^{-3}. For each value of n_e the three cases of the front of T_e mentioned in section 3b are included (the respective maximum values of T_e are 20, 30 and 45 eV). The decrease of T_e due to radiation losses (see section 3b) is practically independent of n_e in the included interval (dependence only due to different ionization states of oxygen) and it is in relatively good agreement with plasma bulk decay observed at diamagnetic measurements [5] as mentioned in introduction. The three resulting time courses of T_e, as calculated for $n_e = 10^{15}$ cm^{-3}, are shown in Fig. 10 - 12. For the above mentioned nine combinations of n_e and T_e we have calculated the time dependent intensities of selected spectral lines of O^{2+} - O^{5+} (see section 3c) and a rough form of bare XRD signal (see section 3a, radiation losses).

The main results of XRD signal calculations are the following: In included interval of plasma parameters (n_e, T_e), the magnitude of bare XRD signal is practically independent of T_e (which is in good agreement with experimental observations on REBEX) and increases linearly with n_e

(and similarly with n_o). For higher temperatures, the plateau of XRD signal near to its maximum value is longer. These facts are illustrated by Fig. 13 - 15, where the XRD signals calculated for ($T_{e\,max}$, n_e) = (20 eV, 5.10^{14} cm^{-3}); (30 eV, 10^{15} cm^{-3}); (45 eV, 2.10^{15} cm^{-3}) are shown, respectively. Some typical properties of signals for different T_e obtained from constant T_e calculations [3] are now masked by the time dependence of T_e. The initial part of the signal ($t < 0{,}5\ \mu s$) can be increased by optically allowed transitions to metastable states of O^{4+} mentioned in section 2. However, this increase represents only some "fine structure" of XRD signal, which can be masked by presence of other impurities. The other results (T_e, lines intensity) cannot be influenced by these transitions, because the front of T_e is gived in an explicit form.

In Fig. 16 - 24 the time dependences of intensities of selected spectral lines of O^{2+} - O^{5+} are shown for all nine above mentioned combinations of n_e and T_e. By taking into account the two typical quantities, namely the relative values of maximum intensity of lines corresponding to different ionization stages and the times of maximum intensities, the individual cases can be sufficiently distinguished. For example, only the measurable intensity of O^{5+} lines and/or substantially predominant intensity of O^{4+} lines indicate $T_{e\,max}$ near to 50 eV. On the other hand, substantially predominant intensity of O^{2+} lines corresponds to $T_{e\,max}$ about 20 eV. More information on time behaviour of T_e can be obtained by measuring electron density in an independent way.

By taking into account the proposed geometrical arrangement of the prepared experiment and the sensitivity of proposed apparatus, and including the fact that only a part of the total impurity density is oxygen, the magnitudes of signals corresponding to the line intensities indicated in Fig. 16 - 24 of the order of (0,1 - 5 mA) can be achieved.

5) Conclusion

At higher plasma densities on REBEX experiment, the measurements of spectral lines intensity can give more information on T_e than XRD-filters measurements because of excluding a series of "free parameters" (accurate chemical composition of impurities, complicated line spectrum), especially by measuring n_e in an independent way. Intensities of selected lines which can be achieved are sufficient for measurements by accessible apparatus. The presented calculations can be used for interpretation of such measurements; for this purpose, other time courses of T_e can be included in our calculation programe when needed. The simultaneously made XRD-signal calculations can be used for check measurements. They can also help to explain some facts of our previous measurements.

In such regimes, when radiation losses are sufficiently dominant mechanism of plasma decay, the time integrated XRD signal obtained in a suitable geometrical arrangement can be used for estimations of energy content of plasma bulk and compared with diamagnetic measurements, which give a total plasma energy content including overthermal electrons and energy of redistributed magnetic field.

Some simplifications in comparison with our constant T_e calculations [3] (only six ionization stages, only one energy level for ionization and radiative recombination, only one resonant transition for dielectronic recombination and radiation losses, neglection of continual spectrum) allow us to reduce the computer time needed for variable T_e calculations to a reasonable degree (one run ~30 minutes on SM 52/11 computer).

6) Acknowledgements

We would like to acknowledge Dr. P. Šunka for many helpful discussions and Dr. J. Ullschmied for comparison of our results with diamagnetic measurements.

7) References

[1] Sunka P.: Proc.16th ICPIG, Duesseldorf 1983, Inv.Pap.,232

[2] Raus J., Piffl V.: Czech J.Phys. B38,11(1988),1222

[3] Raus.J., Babicky V.: Preprint IPPCZ 287, IPP Prague, January 1989

[4] Raus.J., Babicky V.: 14th Czech.Sem. on Plasma Physics and Technology, Liblice, March 1989

[5] Ullschmied J.: 14th Czech.Sem. on Plasma Physics and Technology, Liblice, March 1989

[6] Frish S.E.: Opticheskije spektry atomov, Gos.Izd. Fiz.-Mat.Lit., Moscow-Leningrad 1963

[7] Striganov A.R., Odincova G.A.: Tablici spektralnych linij atomov i ionov, Energoizdat, Moscow 1982

[8] Kelly R.L.: Atomic and ionic spectrum lines below 2000 A, Oak Ridge National Laboratory 1982

[9] Breton C.et.al.: J.Quant.Spectr.Rad.Transfer 19(1978), 367

[10] Tazima T.et.al.: Nucl.Fusion 17(1977),419

[11] von Goeler S.et.al.: Nucl.Fusion 15(1975),301

[12] Lotz W.: Preprint 1/62, IPP Garching, May 1967

[13] Lotz W.: J.Opt.Soc.Am. 58(1968), 915

[14] Vainshtein L.A.: Trudy FIAN 119, Nauka, Moscow 1980,3

[15] Presnyakov L.P.et.al.: Elementarnye procesy s uchastiem mnogozaryadnych ionov, Energoatomizdat, Moscow 1986

Tab.1: Selected lines of oxygen ions.

Q	2	3	4	5
terms λ [Å] trans. 2s-2p	$^3P_0-^3P_1$ 702,332 $^3P_1-^3P_0$ 702,822 $^3P_1-^3P_{1,2}$ 702,899 $^3P_2-^3P_{1,2}$ 703,850	$^2P_{1/2}-^2D_{3/2}$ 787,711 $^2P_{3/2}-^2D_{3/2}$ 790,109 $^2P_{3/2}-^2D_{5/2}$ 790,199	$^1S_0-^1P_1$ 629,730	$^2S_{1/2}-^2P_{3/2}$ 1031,924
W [eV]	17,64	15,71	19,69	12,02
b	4,52	3,77	13,3	2,46

Tab.2: Atomic constants of oxygen ions.

Q	1	2	3	4	5
I [eV]	38,1	59,4	84,2	114	138
ξ	5	4	3	2	1
a	2,2	2,8	3,0	3,0	3,0
E [eV]	14,9	18,5	19,0	19,7	12,0
c	6,8	7,3	8,7	8,3	3,1
d	2,99	6,89	12,6	21,9	12,8

CONSTANT Te CALCULATIONS

Fig.1

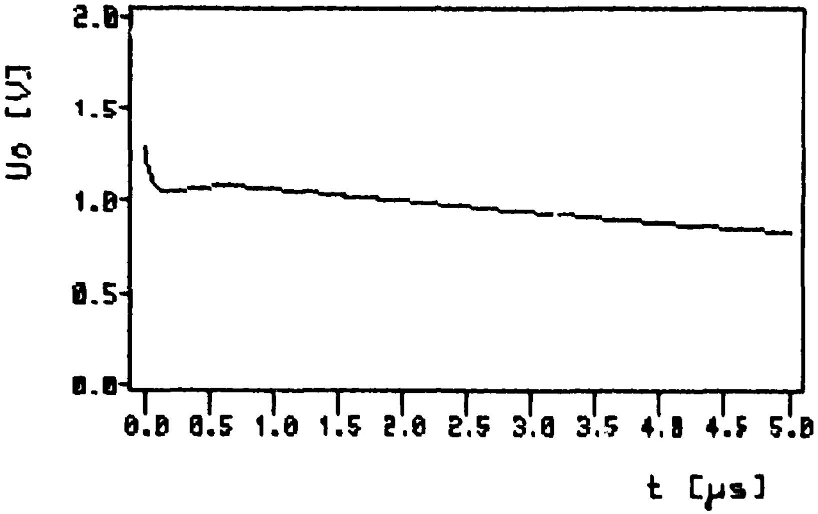

Fig.2

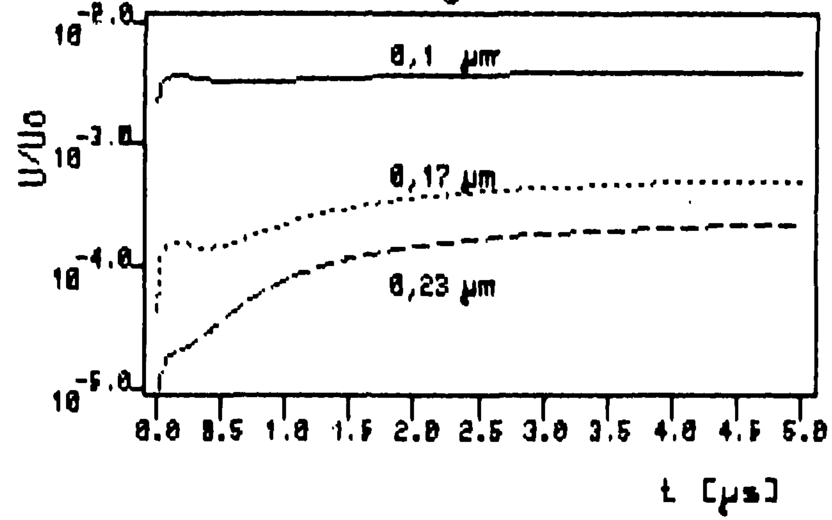

EXPERIMENTAL RESULTS

Fig.3

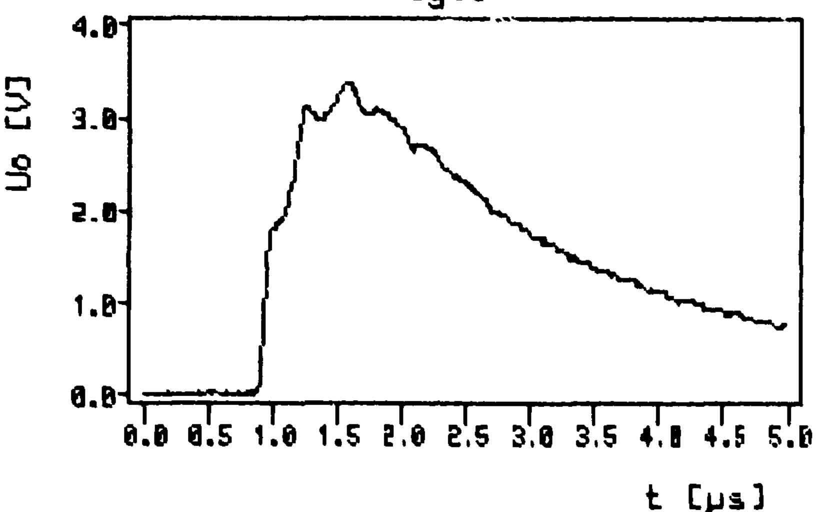

Fig.4

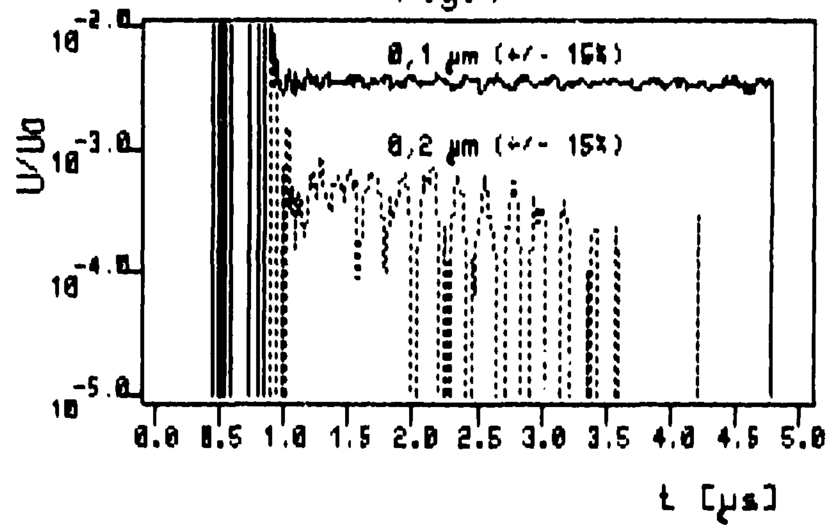

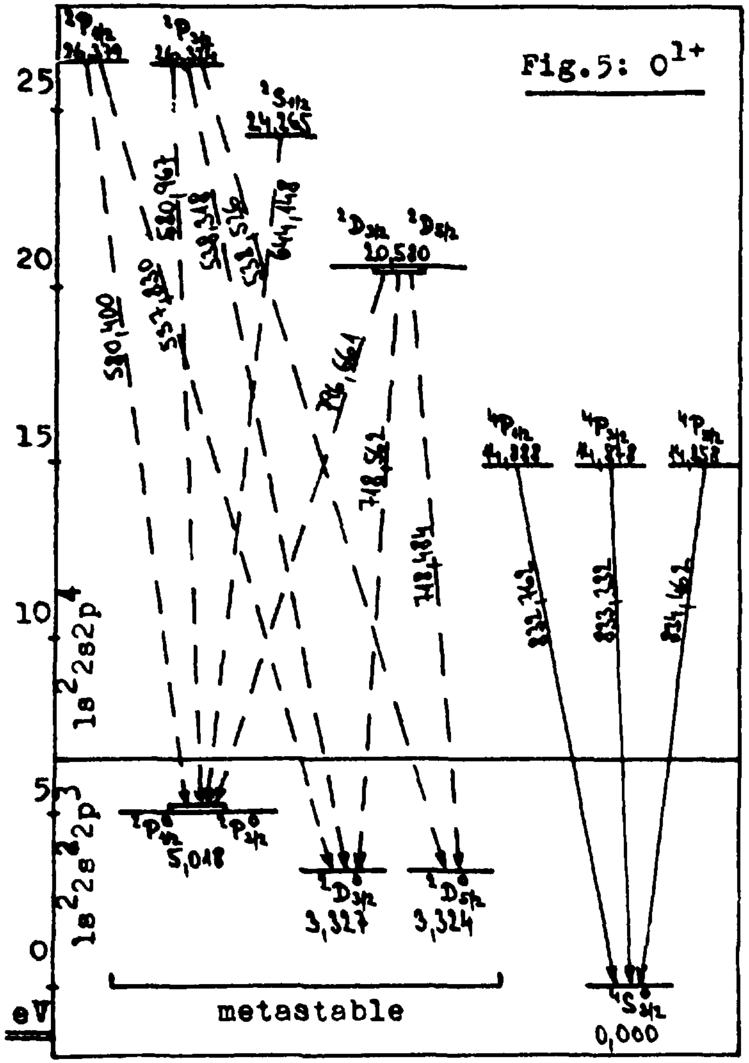

Fig.5: O^{1+}

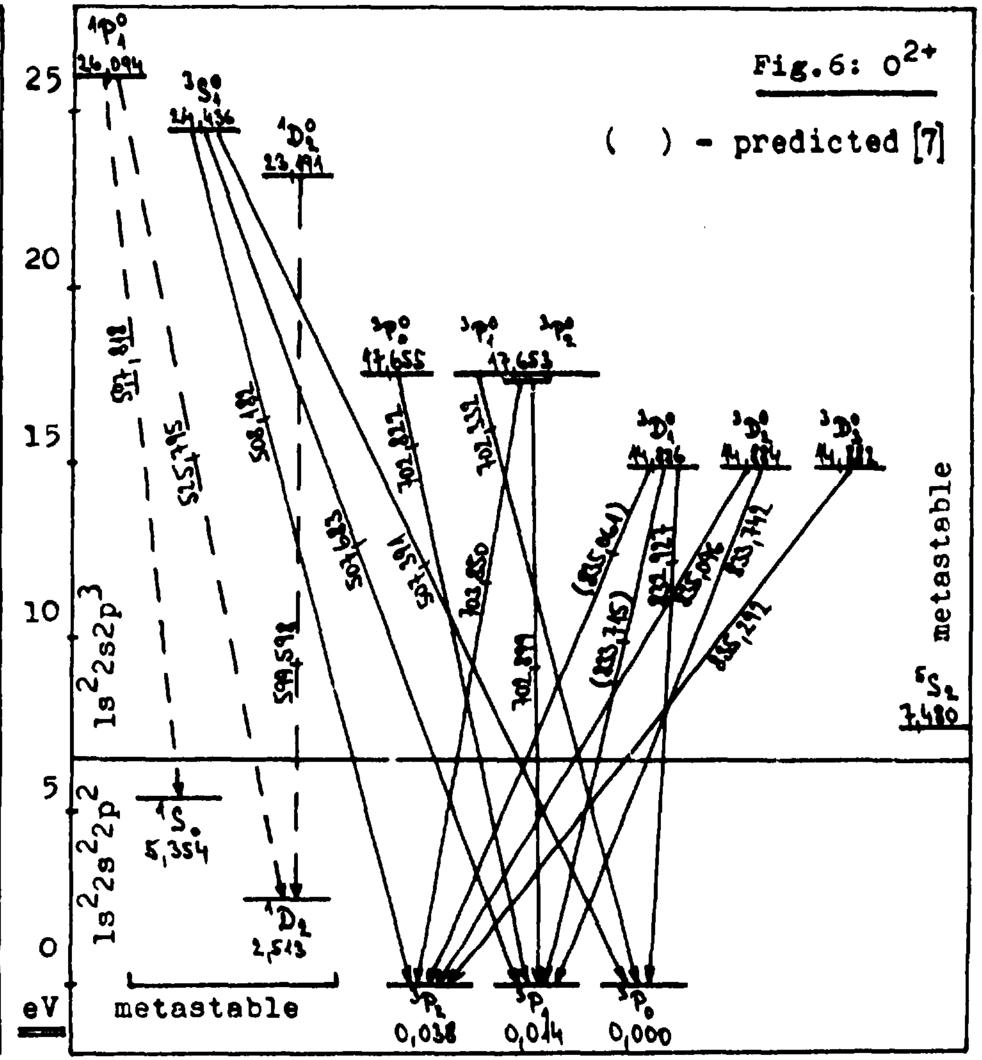

Fig.6: O^{2+}

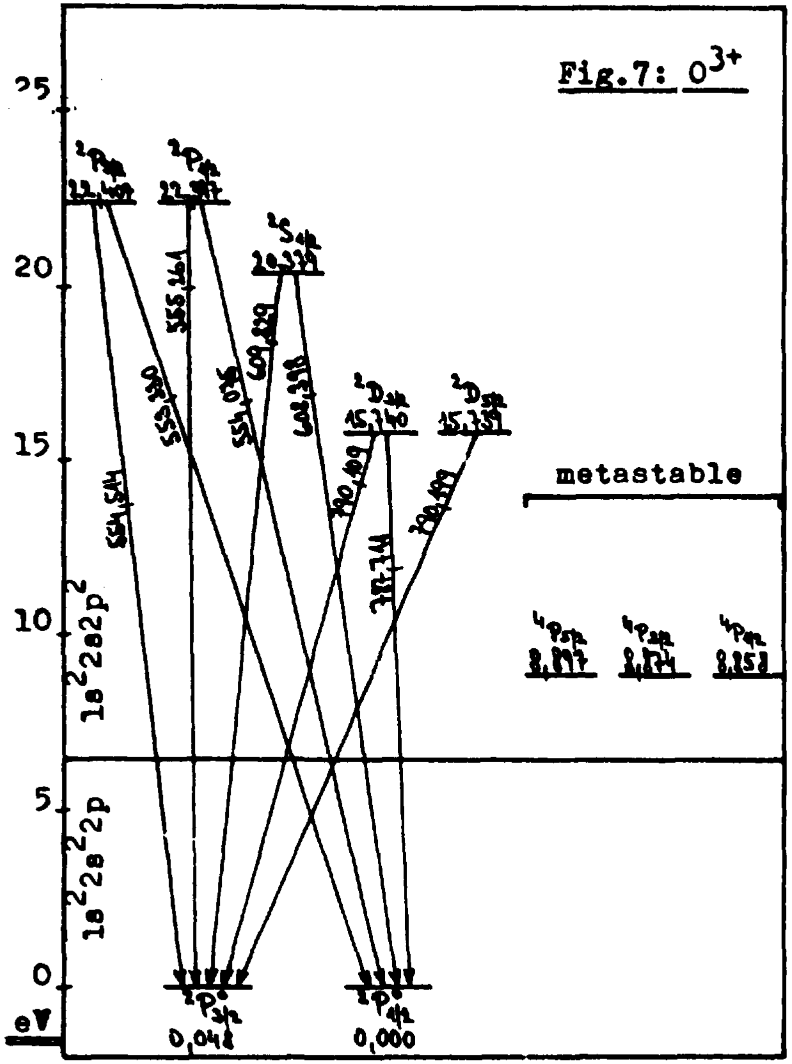

Fig.7: O^{3+}

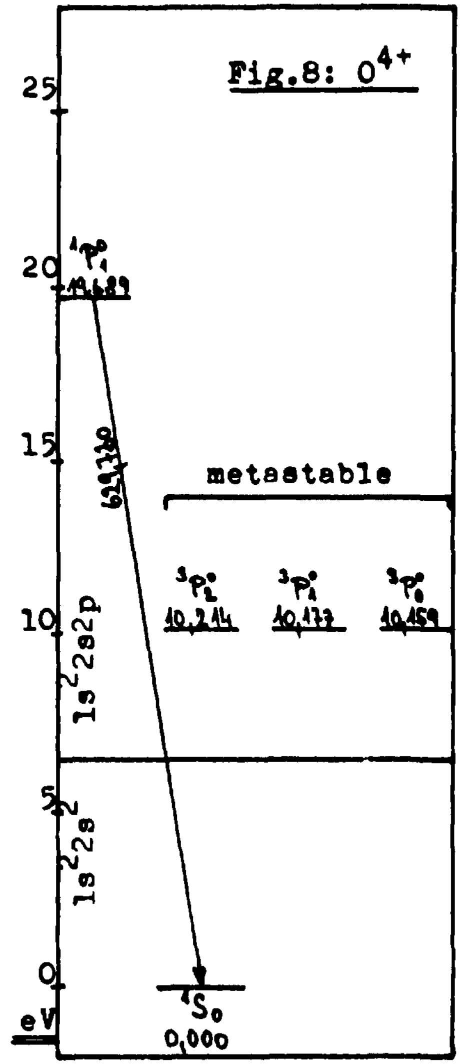

Fig.8: O^{4+}

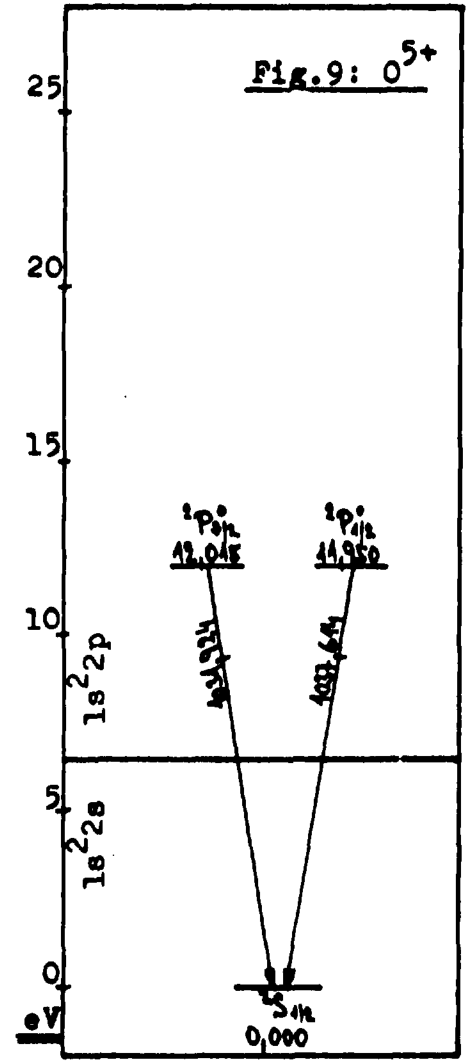

Fig.9: O^{5+}

Fig.10: Te max = 20 eV

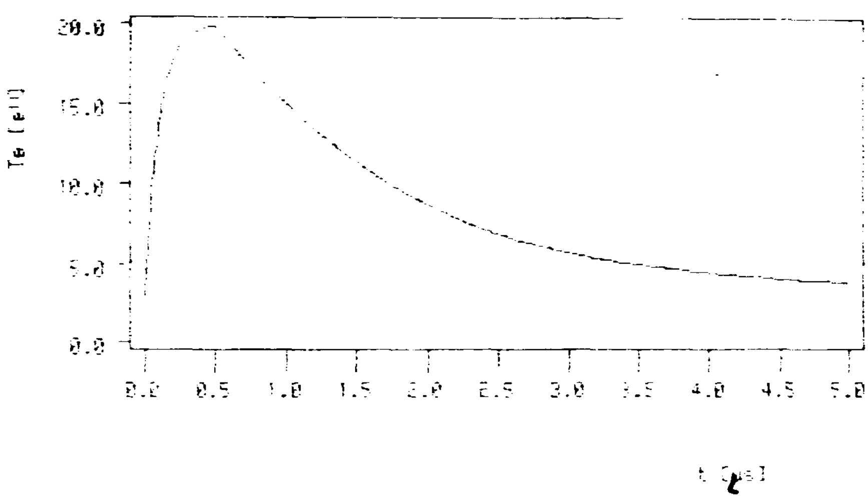

Fig.11: Te max = 30 eV

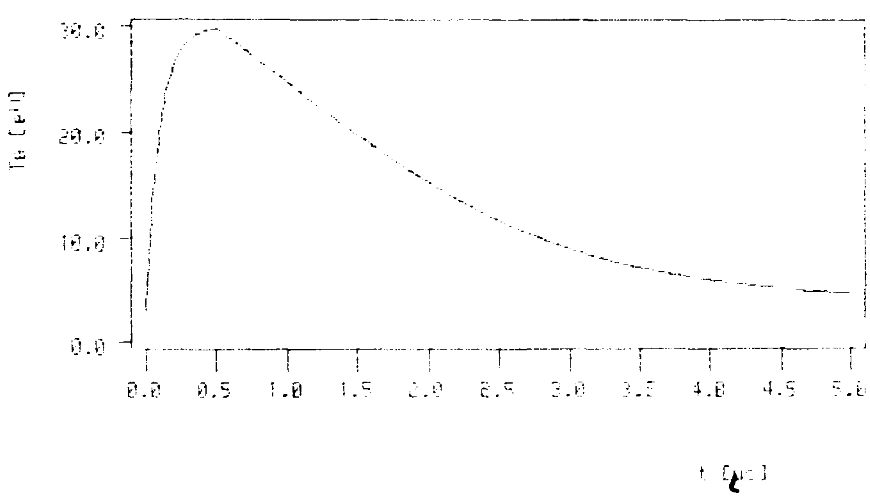

Fig.12: Te max = 45 eV

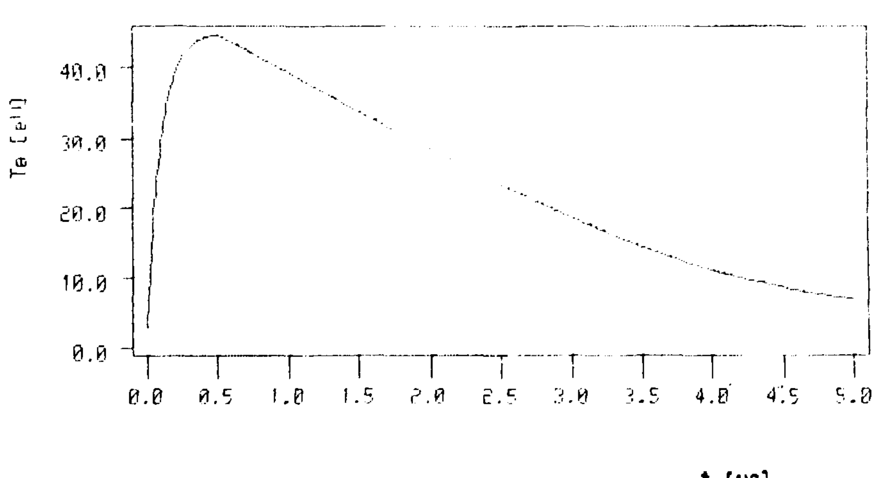

Fig.13: Te max = 20 eV, ne = 5e14 cm-3

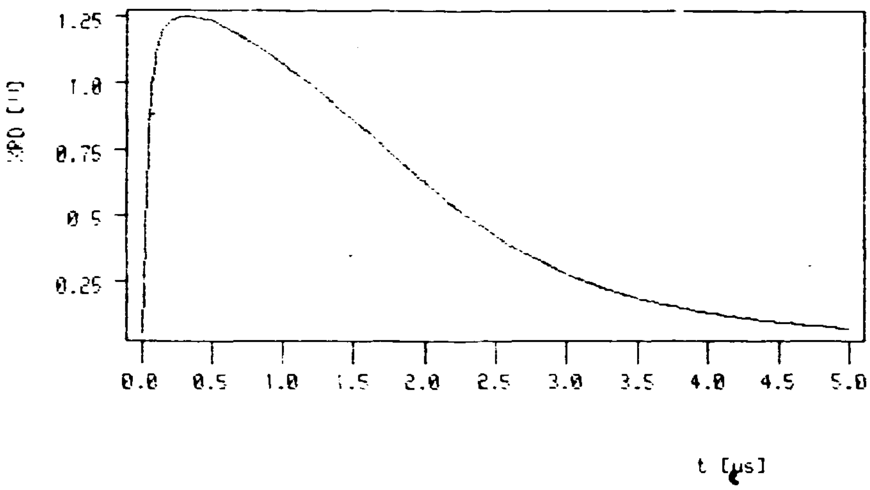

Fig.14: Te max = 30 eV, ne = 1e15 cm-3

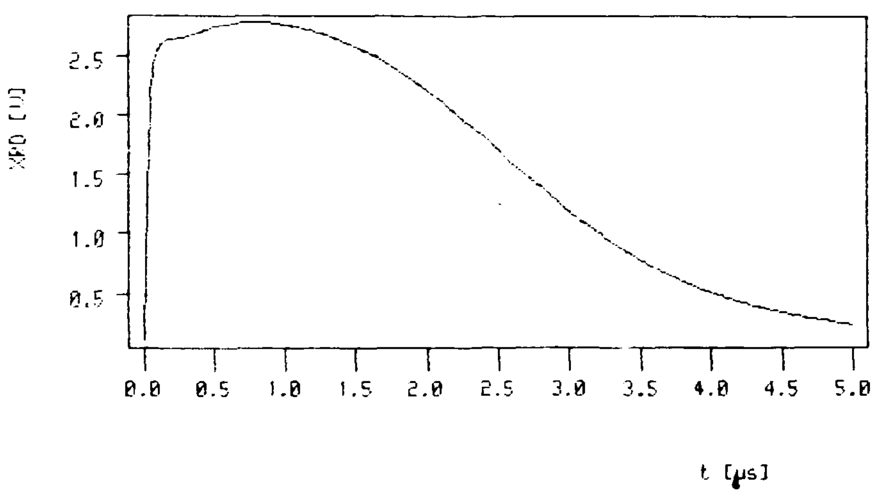

Fig.15: Te max = 45 eV, ne = 2e15 cm-3

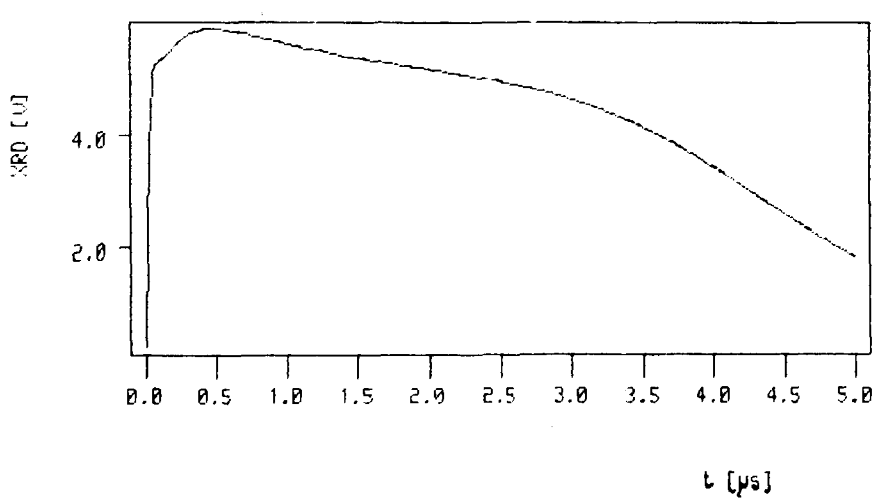

Fig.16: Te max = 20 eV, ne = 5e14 cm-3

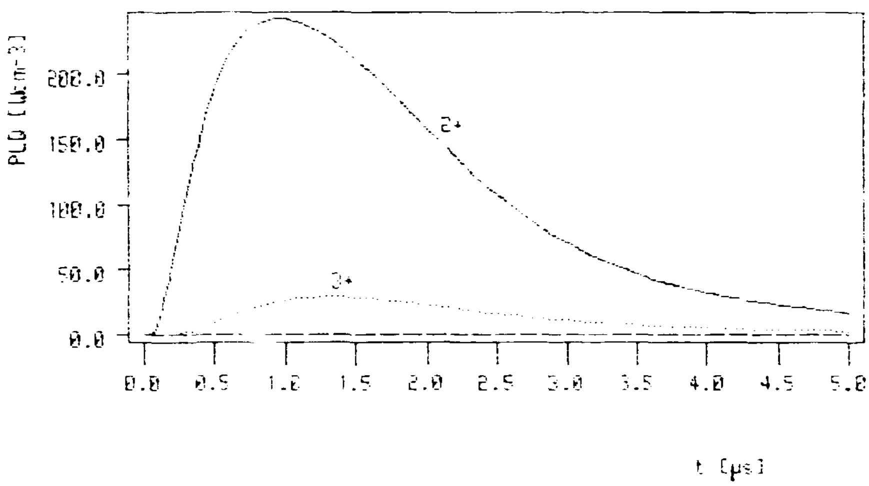

Fig.17: Te max = 20 eV, ne = 1e15 cm-3

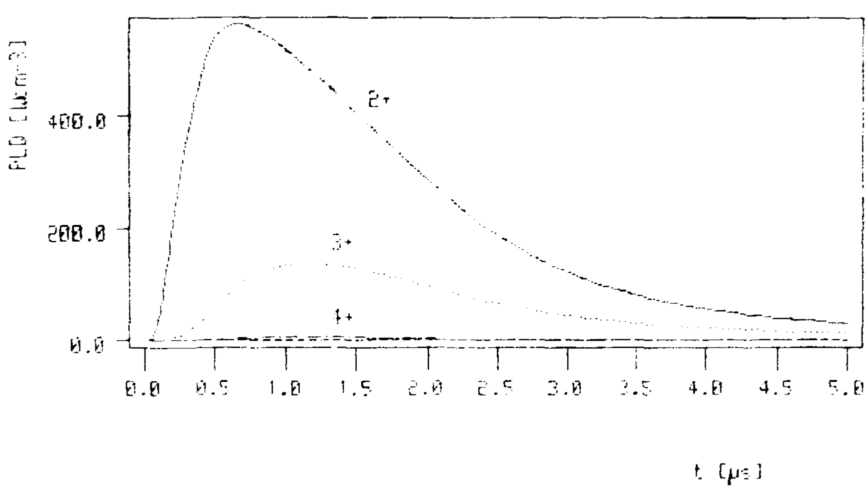

Fig.18: Te max = 20 eV, ne = 2e15 cm-3

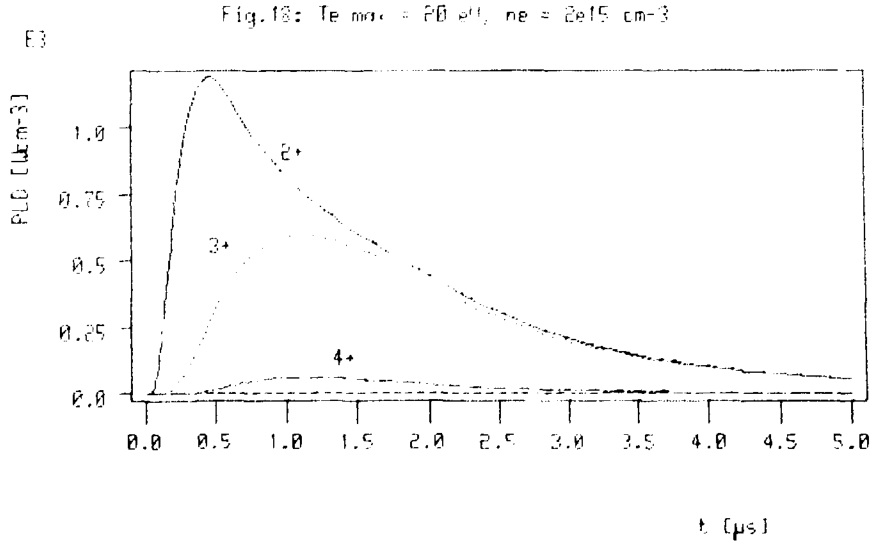

Fig.19: Te max = 30 eV, ne = 5e14 cm-3

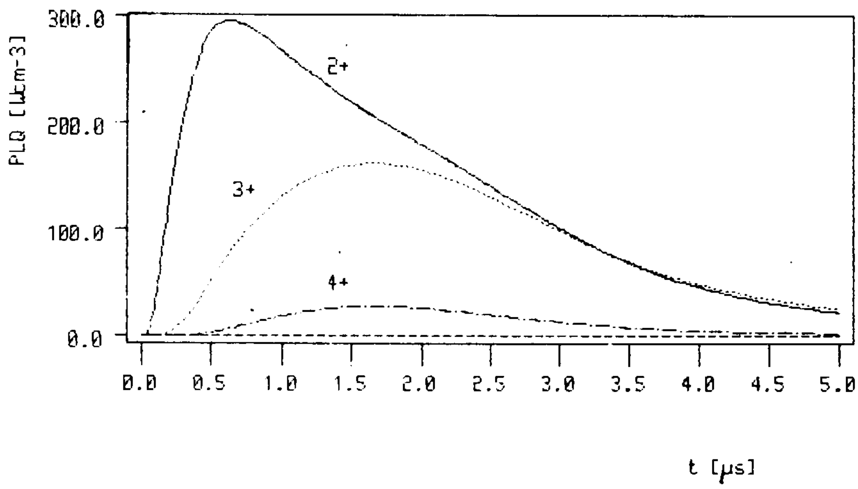

Fig.20: Te max = 30 eV, ne = 1e15 cm-3

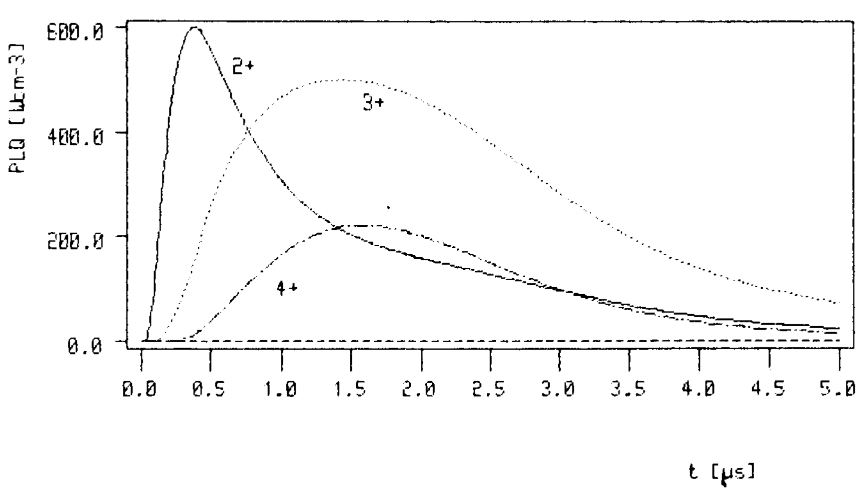

Fig.21: Te max = 30 eV, ne = 2e15 cm-3

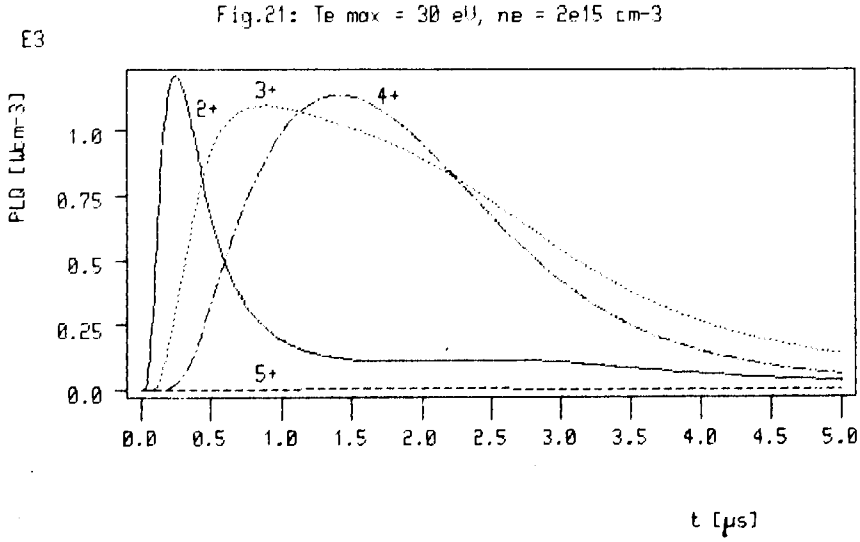

Fig.22: Te max = 45 eV, ne = 5e14 cm-3

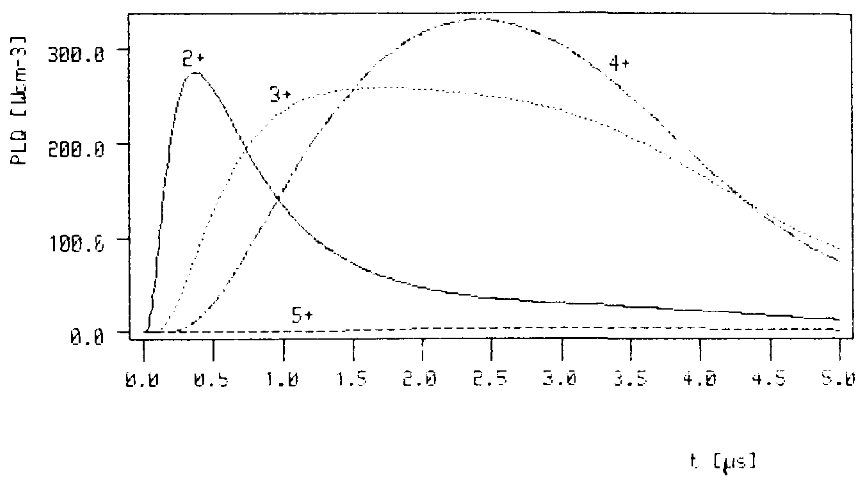

Fig.23: Te max = 45 eV, ne = 1e15 cm-3

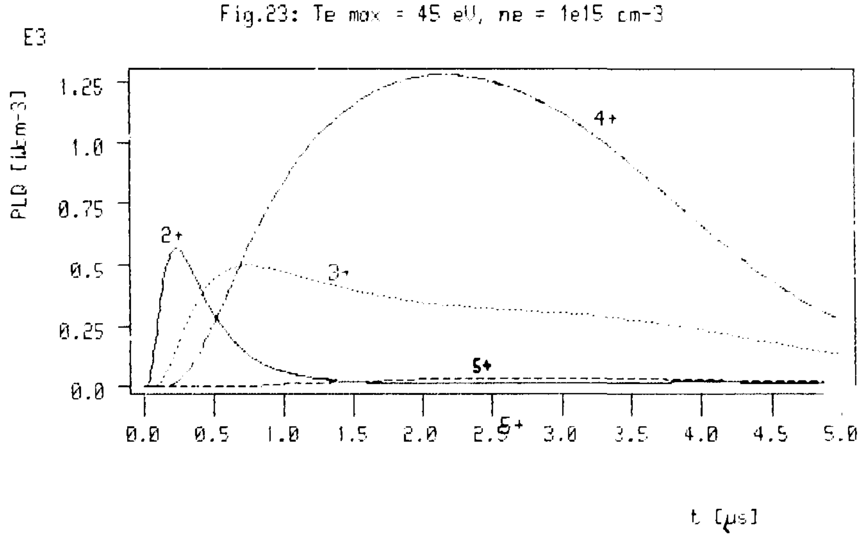

Fig.24: Te max = 45 eV, ne = 2e15 cm-3